Original Article
XIST promote the proliferation and migration of non-small cell lung cancer cells via sponging miR-16 and regulating CDK8 expression

Xiaoyun Zhou*, Xiaohui Xu*, Chao Gao, Yushang Cui

*Department of Thoracic Surgery, Peking Union Medical College Hospital, 1 Shuaifuyuan, Wangfujing, Dongcheng, Beijing 100730, P. R. China. *Equal contributors.*

Abstract: Up-regulation of long non-coding RNA (lncRNA) XIST has been observed in the tissue samples of non-small cell lung cancer (NSCLC), however, the underlying mechanisms remain uncertain. The aim of this study is to investigate the roles of XIST in the pathogenesis of NSCLC and the underlying mechanism. We noted that XIST in NSCLC tumor tissue and cell lines was significantly up-regulated. XIST over-expression promoted the proliferation and migration, meantime, increased the proportion of cells in the S phase in NSCLC cell line A549 and H1299. Meantime, knockdown of XIST showed the opposite effects. In vivo study further revealed a oncogenic effect of XIST. In addition, we conducted bioinformatics analysis and luciferase activity assay to find out the potential target miR of XIST and the potential target gene of miR-16 which is CDK8. In conclusion, our findings proved that XIST can serve as a tumor promoter in the pathogenesis of NSCLC, suggesting that XIST has the potential to become a novel therapeutic target for the treatment of NSCLC.

Keywords: XIST, miR-16, CDK8, proliferation, migration, non-small cell lung cancer cells

Introduction

Lung cancer is the most prevalent cancer which remain the leading cause of cancer-related death worldwide [1, 2]. Non-small cell lung cancer (NSCLC) accounts for more than 80% of lung cancers [3, 4]. While major progress has been made in NSCLC diagnostics and therapy, the 5 year survival rate of NSCLC is less than 20% for their advanced stage diagnosed, poor prognosis phase, bad predictions, recurrence and chemo-chemical resistance [5]. Thus, developing novel screening methods and early biomarkers for the diagnose and treatment of NSCLC is of great importance which depends on the deep understanding of the pathophysiological mechanisms contributing to the progress of NSCLC.

Long non-coding RNAs (lncRNAs) are a group of non-coding RNA longer than 200 nucleotides [6]. The regulatory roles of lncRNA were on post-transcriptional level like other types of non-coding RNAs, for instance, microRNAs and circular RNAs [7, 8]. In the latest years, many lncRNA researches have become commonly recognized for involvement in various biological processes such as proliferation, migration, apoptosis, angiogenesis, embryo development and tumorigenesis [9-12]. Several recent studies have demonstrated the altered expression of lncRNAs in NSCLC tumor tissues and the adjacent tissues including XIST. They observed that XIST was significantly up-regulated in NSCLC. Further investigation indicated that XIST promoted cell viability, invasion, epithelial-mesenchymal transition (EMT) and decrease chemosensitivity of NSCLC [13-18]. Interestingly, low expression of XIST in tissue samples of patients with NSCLC may indicate better prognosis. XIST has been identified as a onco-lncRNA in NSCLC. However, it is continues to be further explored the fundamental mechanism for XIST's involvement in NSCLC pathogenesis.

MiRNAs are also a group of non-coding RNAs that are 22-28 oligonucleotide-long and regulate gene expression by base pairing with the

3'untranslated region (3'-UTR) of the target genes at post-transcriptional level, thus, involved in a number of cell physiological process [19, 20].

In the present study, we have performed both clinical and *in vitro* cellular analysis to investigate the roles of XIST in NSCLC. First, we compared the expression of XIST in NSCLC tumor tissues and the adjacent tissues. Further, the effect of XIST on the proliferation and migration of NSCLC cancer cells and the underlying mechanism were also examined. Our results proved that XIST is tumor promoter in NSCLC and provided a potential novel therapeutic target for treating NSCLC.

Methods

Patients and clinical tissue samples

A pair of 15 of NSCLC and adjacent normal tissue samples were obtained from NSCLC patients in Peking Union Medical College Hospital between 2017 and 2019. All patients were diagnosed as NSCLC pathologically, and patients who have the history of preoperative radio and/or chemotherapies were excluded from this study. The tissue samples were quick freezed in liquid nitrogen after surgery and stored in -80°C. The informed consent was obtained from each patient. This study was approved by the ethical committee of Peking Union Medical College Hospital.

Cell culture

Human NSCLC cell lines A549, H1299, H292 and H460 were purchased from Shanghai Institutes for Biological Sciences (Shanghai, China) and the normal lung mucosa cell line HBE was purchased from INCELL (San Antonio, TX, USA). Cells were maintained in RPMI-1640 medium (Invitrogen, USA) supplied with 10% of FBS (fetal bovine serum, Invitrogen, Carlsbad, CA, USA) at 37°C in an incubator (with 5% CO_2 humidified).

Transfection and treatment

XIST siRNA and XIST over-expression plasmid were synthesized by Shanghai GenePharma Co.,Ltd (Shanghai, China). A549 or H1299 cells were transfected with XIST siRNA or XIST over-expression plasmid using lipofectamine 3000 (Invitrogen, Carlsbad, CA, USA) following the manufacturer's protocol. Transfection efficiency was determined by RT-qPCR.

Reverse transcript PCR and quantitative real-time PCR

Total RNAs were extracted from cells or clinical tissue samples using TRIzol reagent (Invitrogen, Carlsbad, CA, USA). The total RNAs weren then reverse transcribed into cDNAs by PrimeScript RT Master Mix (Takara, Dalian, China). Next, quantitative real-time PCR (RT-qPCR) was performed to detect the expression levels of XIST using a SYBR premix Ex Taq kit (Takara, Dalian, China) and on the ABI Biosystems (ABI, CA, USA). The relative expression level of XIST was normalized by $2^{-\Delta\Delta Ct}$ method. GAPDH has been applied for normalization. The real time PCR reactions were performed with the following thermo profiles: 95°C for 30 seconds, 40 cycles of 95°C for 5 seconds and 60°C for 30 seconds.

Cell proliferation analysis

The effect of XIST on cell proliferation were determined by Cell Counting Kit-8 (CCK-8) kit (Beyotime, Shanghai, China) according to the manufacturer's instructions. Briefly, at different time point after transfection, A549 or H1299 cells were washed with PBS (pH 7.4), trypsinized and seeded onto 96-well plates. Then 10 μl of the CCK-8 solution was added to each well followed by incubating at 37°C for 4 hours. The viability of the cells in each well was evaluated through detecting the absorbance at 450 nm using a microplate reader.

Flow cytometry assay

At 72 h after transfection, A549 and H1299 cells were collected, re-suspended in 500 μl binding buffer and stained with 2.5 μl propidium iodide (PI). The cell cycle of the cells was then determined with FACSCalibur system (BD Biosciences, San Jose, CA).

Transwell assay

Transwell assay was performed using transwell chambers (Corning Inc., Corning, USA). A549 or H1299 cells were seeded onto the upper of the chamber of the transwell with the density of 5 × 10^4 cells/well and placed on 24-well plates. After 24 h of incubation at 37°C, cells invaded into the membrane of the lower chamber were

fixed in methanol, stained with crystal violet and photographed by a microscope.

Western blot

The total proteins were isolated from the cells using protease inhibitor cocktail. Protein concentration was examined by BCA protein assay kit (Beyotime, Shanghai, China). Then 40 μg of proteins were loaded onto 10% SDS-PAGE (sodium dodecyl sulfate polyacrylamide gel electrophoresis) gels. When the process of gel electrophoresis was accomplished, the proteins were transferred onto polyvinylidene fluoride (PVDF) membranes and then blocked in 5% non-fat dry milk in Tris-buffered saline (pH 7.4) containing 0.05% Tween 20. Subsequently, the membranes were incubated with the primary antibodies at 4°C overnight. GAPDH was served as the internal control. In the following day, the membranes were incubated with secondary antibodies at room temperature for 2 hours, washed and incubated with chemiluminescent reagent BeyoECL Plus (Beyotime, Shanghai, China). The signals were detected and photographed by Tanon 6100 Chemiluminescent Imaging System (Tanon, Shanghai, China).

Immunohistochemical staining (IHC)

The tumor tissues were fixed in 4% paraformaldehyde for 24 h, dehydrated in a graded alcohol series and embedded in paraffin followed by cutting into 5 μm sections. The sections were deparaffinized, rehydrated with a graded alcohol series and then incubated in 96°C 0.01 mol/l sodium citrate buffer for the antigen retrieval. After incubation in 5% H_2O_2, was applied for quenching endogenous peroxidase activity. The sections were blocked with 10% non-immune goat serum to reduce non-specific binding. The sections were incubated with primary antibody overnight at 4°C. Immunostaining was performed using streptavidin-peroxidase and diaminobenzidine (DAB) according to the manufacturer's instructions (Beyotime, Shanghai, China). The sections were mounted with gummi after staining the nucleus with hematoxylin.

Luciferase activity assay

The wild-type or mutant sequence at the predicted 3'UTR region of XIST were synthesized and cloned into the pGL3 Luciferase Reporter Vectors (Promega, CA, USA) at the KpnI and BamHI sites. A549 and H1299 cells were co-transfected with miR-16 mimics or mimic control along with pGL3 vectors containing the wild type or mutant targeting region of XIST. TRL-SV40 plasmid (Promega, CA, USA) was transfected as a internal control. The cells were harvested and subsequently measured the luciferase activity using the Dual-Luciferase Assay kit (Promega, WI, USA) at 48 h after transfection.

Xenograft model

A total number of 3×10^6 A549 cells were harvested and resuspended in 100 μL DMED medium. The nude mice were injected with cells infected with XIST overexpressed or deleted A549 cells along with there negative control respectively at the posterior flank. The length (L) and width (W) of tumor were measured with calipers every 3 days. After 28 days, the tumors were excised out from the sacrificed mice and weighed.

Colony-formation assay

The cells treated with indicated conditions were seeded in 12-well plates (100/well). After incubated for 2 weeks, crystal violet (0.05%, Beyotime, Shanghai, China) was used to stain the clonies. Colonies containing more than 50 cells were counted.

Statistical analysis

All data are presented as the means ± standard deviation (SD). The statistical analyses were performed using one-way ANOVA and Student's test. The data were analyzed using GraphPad Prism 5.0 and $P < 0.05$ was considered to be statistically significant. All experiments were performed independently triplicates.

Results

Up-regulation of XIST in non-small cell lung cancer tissues and cell lines

QPCR was used to evaluate the expression levels of XIST in NSCLC tissues and the adjacent normal tissues as well as NSCLC cell lines and normal lung epithelial cell line HBE. We observed that XIST was up-regulated notably in
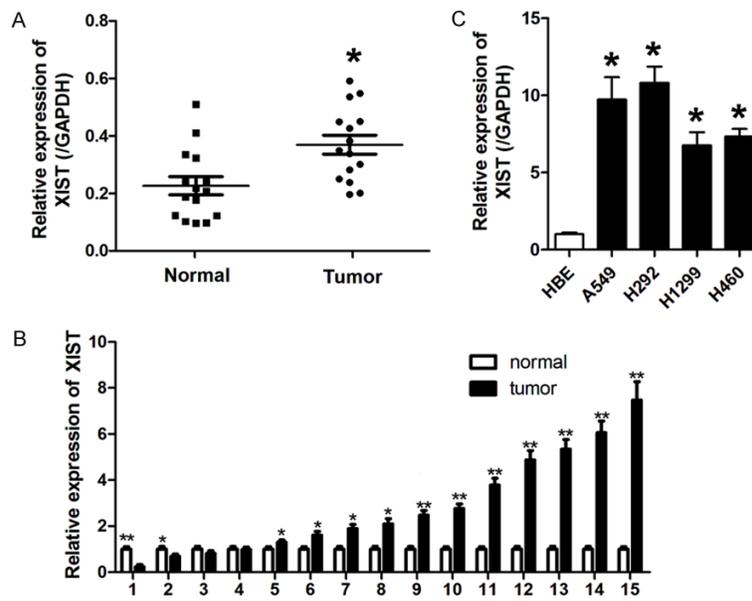
Figure 1. XIST was up-regulated in NSCLC tissues and cell lines. A, B. Expression of XIST in NSCLC tissue specimens and adjacent normal tissues were determined by a qRT-PCR assay, the level of XIST was up-regulated in NSCLC tissues. C. Expression of XIST in NSCLC cells and normal colonic mucosa cells were determined by a qRT-PCR assay, the level of XIST was up-regulated in NSCLC cell lines including A549, H292, H1299 and H460. *P < 0.05 versus normal or HBE group.

nude mice model was established though subcutaneously injecting genetically modified A549 cells. As expected, compared with control group, XIST overexpression significantly promoted the tumor growth of non-small cell lung cancer and knock down of XIST inhibited the tumor growth as shown in the tumor growth curve (**Figure 3A-C**). QPCR was performed to evaluate the XIST expression level in the tumor tissues indicating the success of over-expressing or knocking down of XIST (**Figure 3D**). IHC assay was used to detect the expression of ki67 which is a marker of the cell proliferation. We found that ki67 was significantly up-regulated in the XIST treatment group and down-regulated in si-XIST treatment group (**Figure 3E**).

the NSCLC tissues and cell lines in comparison with the normal tissues and HBE cell (**Figure 1A-C**).

XIST promoted the proliferation, migration and induced G0/G1 arrest of non-small cell lung cancer cells

To determine the function of XIST in non-small cell lung cancer, we carried out loss and gain of function study. We observed that XIST over-expression was capable of promoting the proliferation, migration and colony formation ability of non-small cell lung cancer cell. In addition, the proportion of cells in the S phase was increased by XIST over-expression compared to the control group. In contrast, we found that knock down of XIST by transfection of siRNA of XIST significantly inhibited the proliferation, migration and colony formation ability of non-small cell lung cancer cell. Meantime, XIST knock down notably decreased the proportion of S phase in NSCLC cells (**Figure 2A-D**).

XIST promoted tumor growth of non-small cell lung cancer

In order to elucidate the role of XIST in the regulation of non-small cell lung cancer, xenograft

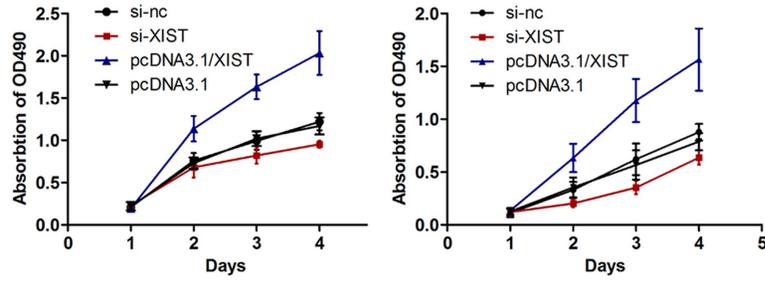*MiR-16 was down-regulated in non-small cell lung cancer and directly target XIST*

LncRNA was able to sponge miRNAs to regulate the gene expression and cell process. Thus, we predicted the potential targeting miRs of XIST using bioinformatics analysis. **Figure 4A** showed the potential target region between XIST and miR-16. To verify whether miR-16 directly target XIST in NSCLC cell, luciferase activity assays was performed. The results revealed that miR-16 notably reduced the luciferase activity in A549 and H1299 cells co-transfected with pGL3-wild-XIST but not the pGL3-mut-XIST (**Figure 4B**). QPCR analyses further confirmed that miR-16 reduced the RNA expression of XIST (**Figure 4C**) and it was significantly down-regulated in both NSCLC tissue and cells (**Figure 4E**, **4F**). Pearson analysis revealed a negative correlation between XIST and miR-16 (**Figure 4D**).

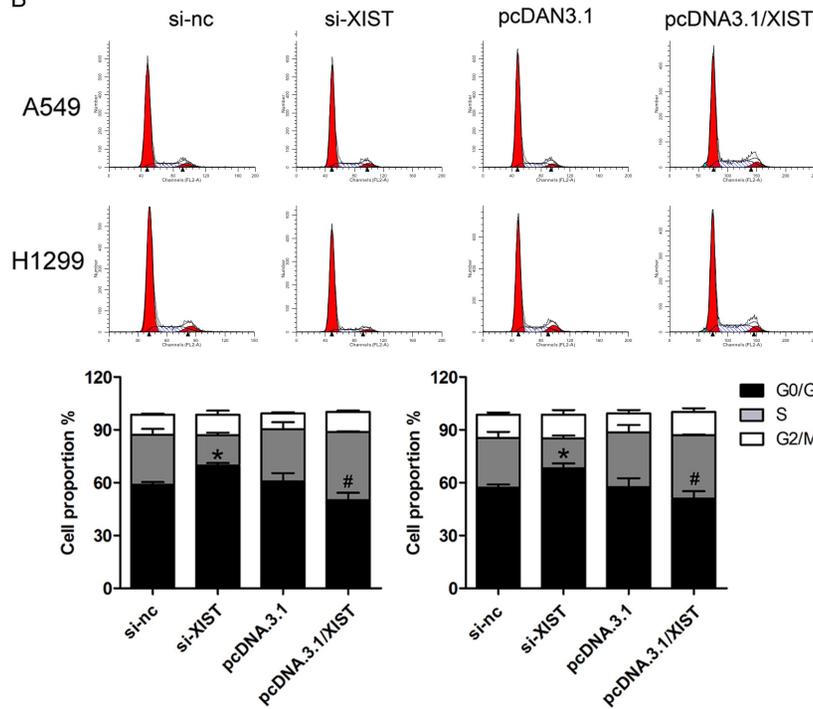*MiR-16 reversed the effect of XIST in NSCLC cells*

In order to further confirm the relation between miR-16 and XIST. We carried out rescue experiment. Cell proliferation, migration, cell cycle and clone formation ability were investigated.

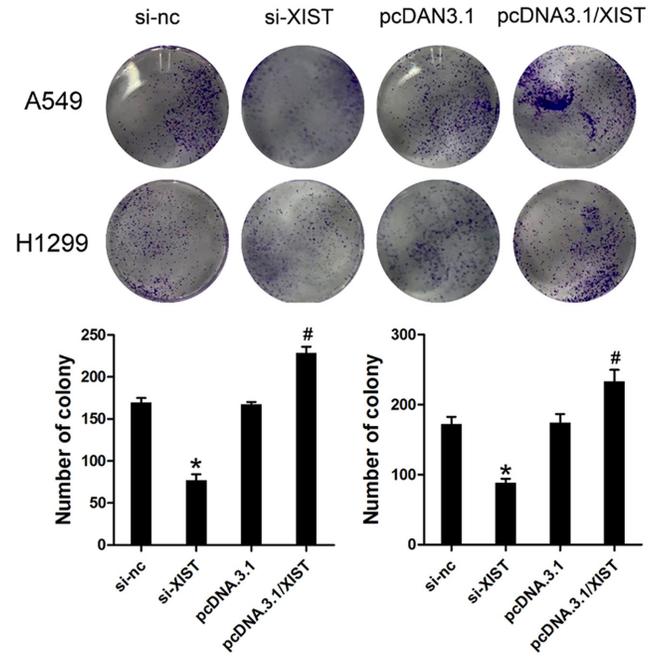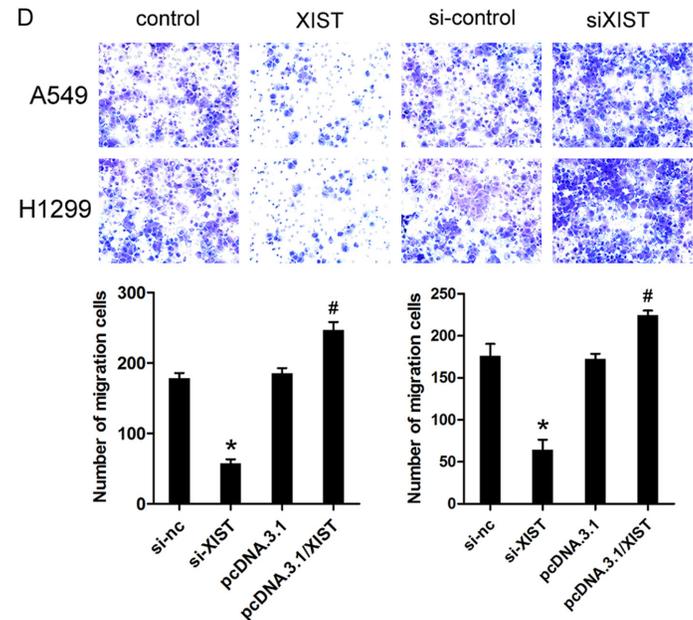Figure 2. XIST promoted tumor growth of non-small cell lung cancer cells. A. A549 and H1299 cells were used in the function study. After transfection of over-expressing and knock down vetor of XIST. CCK-8 assay was carried out to detect the proliferation of NSCLC cells. B. PI staining and flow cytometry was used to detect the cell cycle of NSCLC cells. C. Colony formation assay was performed to evaluate the clone-forming capability of NSCLC cells. D. Transwell assay was performed to detect the migration of NSCLC cells. *P < 0.05 versus si-control group, #P < 0.05 versus pcDNA3.1 group.
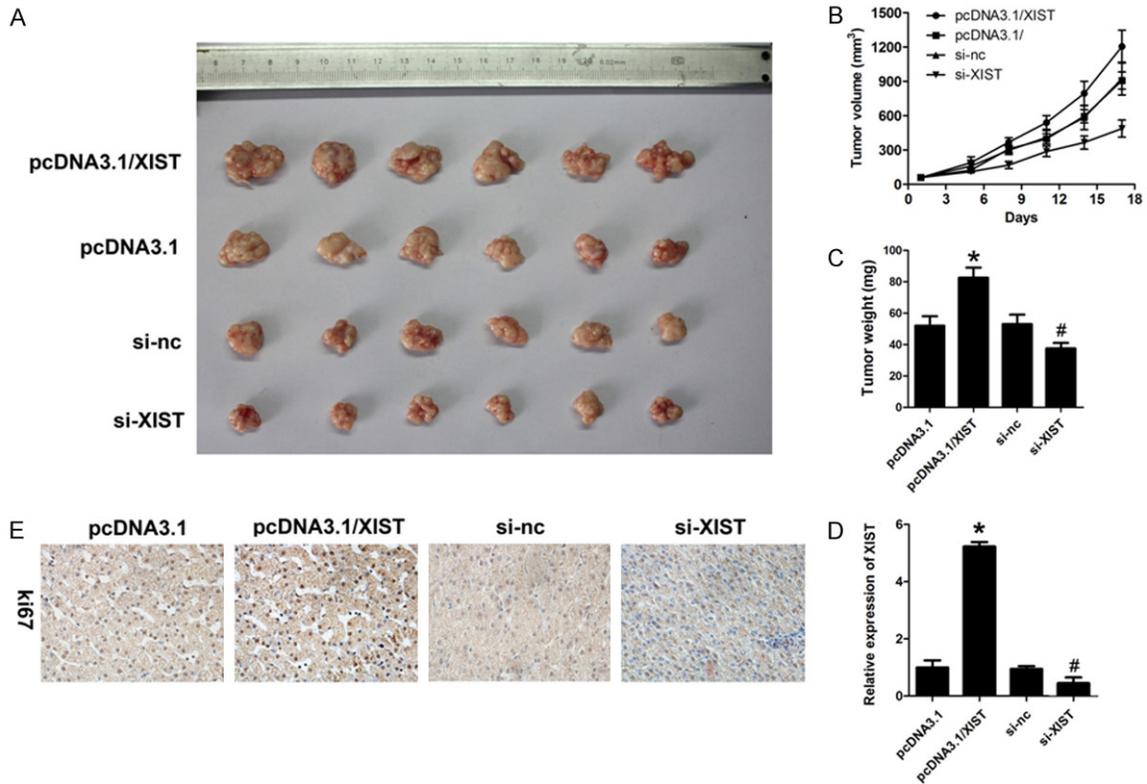

Figure 3. XIST promoted tumor growth of non-small cell lung cancer in vivo. Stable cell line overexpressing and knocking dwon XIST was used to establish xenograft model. A. Representative images of nude mice and tumors from implanted mice. B, C. The tumor volume and weight were measured in different groups. D. Expression level of XIST in tumor tissues were evaluated by qPCR. E. IHC assay was used to detect the expression of ki67 which is a marker of the cell proliferation. *P < 0.05 versus pcDNA3.1 group group, #P < 0.05 versus si-control group.

The results indicated that miR-16 over-expression significantly reversed the effect of XIST on promoting the growth of NSCLC cells (**Figure 5A-D**).

MiR-16 directly targets CDK8 in NSCLC cells

To further elucidate the molecular mechanism underlying the effect of XIST in NSCLC cells. We focused on the downstream target gene of miR-16. Interestingly, we found that CDK8 was a potential target of miR-16 (**Figure 6A**). Luciferase activity assay and qPCR detection verified out prediction (**Figure 6B**, **6C**). Western blot was performed to detect the protein level of CDK8 after over-expression of miR-16. The

results indicated that miR-16 inhibited the protein expression of CDK8 (**Figure 6D**). We next evaluate the level of CDK8 in the NSCLC tissues and cell lines. The IHC (**Figure 6E**) and qPCR (**Figure 6E-G**) results indicated that CDK8 was notably up-regulated in NSCLC tissues and cell lines. The person analysis indicated a negative correlation between miR-16 and CDK8, in addition, a positive correlation between XIST and CDK8 (**Figure 6H**, **6I**).

Discussion

XIST has been studied in a number of cancers including NSCLC. In the current study, we confirmed that the level of XIST was increased in
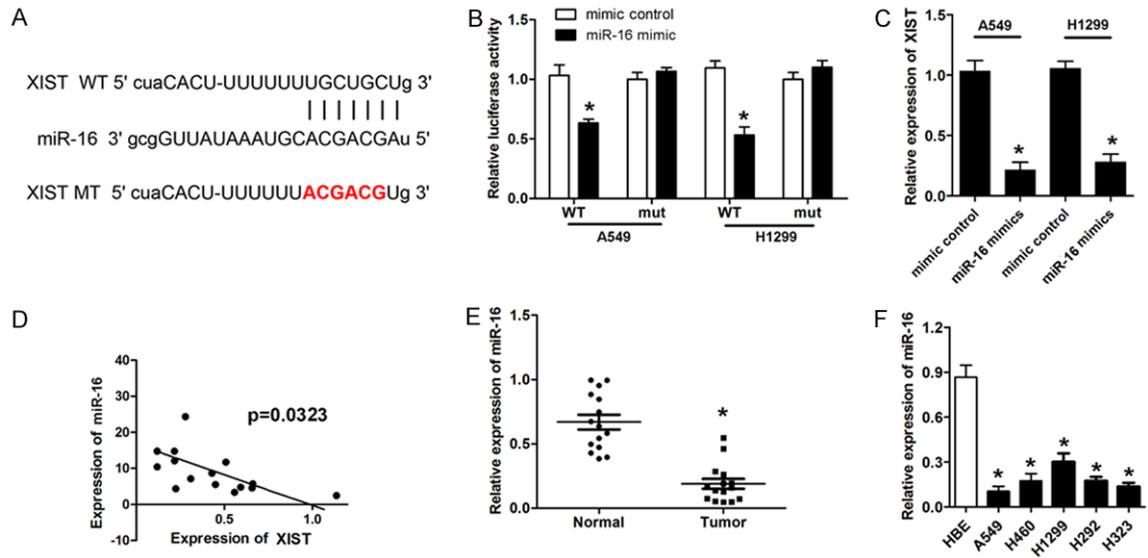
Figure 4. XIST is the direct target of miR-16. A. Prediction of binding sites for XIST and miR-16 by Targetscan. B. NSCLC cells were transfected luciferase reporter vector with wild or mutant type of targeting region along with miR-16 mimic or mimic control. Luciferase activity assay was used to determine whether miR-16 target XIST. C. qPCR was used to detect the XIST level in different groups. D. The correlation analysis was performed between XIST and miIR-16 expression levels. E, F. QPCR was used to evaluate the expression level of XIST in NSCLC tissues and cell lines. *$P < 0.05$ versus normal/mimic control/HBE group.

the NSCLC tissue and cell lines compared to the adjacent normal tissues and normal lung epithelial cells. Consistent with the previous studies which indicating XIST as an oncogene in NSCLC cells. Our findings confirmed that XIST promoted the proliferation and migration of NSCLC cell. In addition, we firstly demonstrated that XIST induced the G0/G1 cell cycle arrest of NSCLC cells which further clarified its function.

lncRNA XIST (X-inactive specific transcript) is a product of the XIST gene and the master regulator of X inactivation in mammals which has been widely investigated in a number of disease especially in cancers. However, the molecular mechanism underlying the function of XIST remain complicated. LncRNAs was capable of directly interacting with the DNAs, RNAs and even proteins to change their conformation, stability or expression levels. Among these, ceRNA mechanism has been most wildly studied as a molecular sponges for microRNAs through their binding sites. It is well documented that alterations in miRNA expression play a critical role in cancer initiation and development. A growing number of studies have suggested the existence of a widespread interaction network involving ceRNAs, in which the ncRNAs can regulate miRNAs by binding to and

titrating them off their binding sites on protein coding messengers.

XIST has been demonstrated to be the sponge for miR-497 [21], miR-92b [22], miR-152 [23]. As in lung cancer, XIST is capable of targeting miR-367/141 [24], miR-139 [25] and miR-186-5p [26]. In our present work, we found a novel target of XIST which is miR-16. MiR-16 was reported to inhibited proliferation, invasion and EMT of NSCLC [27-29]. We found that XIST could significantly inhibit the expression of miR-16. Luciferase activity assay and rescue experiments verified our speculation that miR-16 could directly target XIST in NSCLC cells.

Accumulative evidence have indicated that lncRNAs participate in regulating their downstream genes by acting as ceRNAs. We further predicted and confirmed that miR-16 also targeted CDK8 in NCSLS cells which was firstly reported. The positive correlation between CDK8 and XIST indicated a ceRNA relationship between them. CDK8 has been first linked to cancer when it was identified as an oncogene that is frequently amplified or over-expressed in colon carcinoma [30]. After there, the oncogenetic role CDK8 have been found in colon, breast, and prostate cancers [31-34]. As a
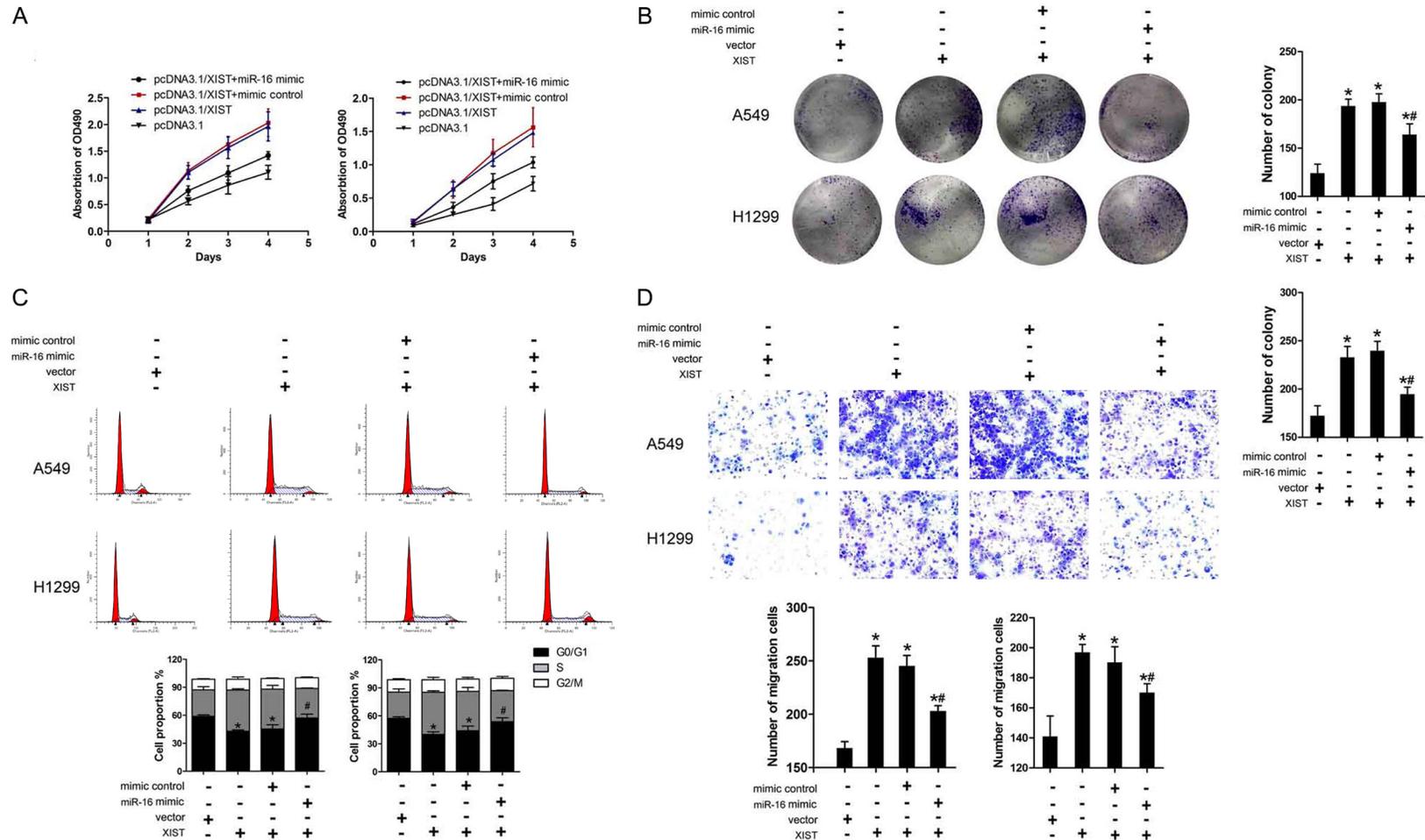
Figure 5. MiR-16 overexpression reversed the effect of XIST in NSCLC cells. NSCLC cells were transfected with XIST overexpressing vector or vector control along with miR-16 mimic or mimic control. A. CCK-8 assay was carried out to detect the proliferation of NSCLCs cells. B. Colony formation assay was performed to evaluate the clone-forming capability of NSCLC cells. C. PI staining and flow cytometry was used to detect the cell cycle of NSCLC cells. D. Transwell assay was performed to detect the migration of NSCLC cells. *P < 0.05 versus vector group, #P < 0.05 versus XIST+mimic control group.
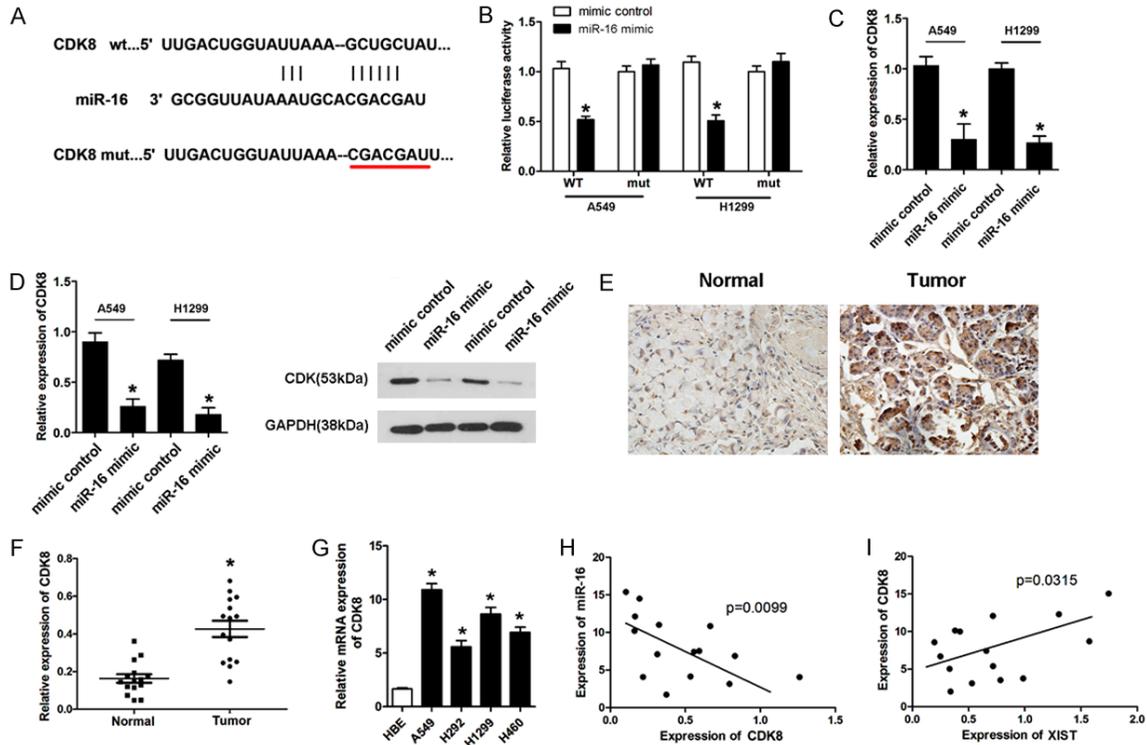
Figure 6. MiR-16 directly targets CDK8 in NSCLC cells. (A) Prediction of binding sites for CDK8 and miR-16 by Targetscan. (B) NSCLC cells were transfected luciferase reporter vector with wild or mutant type of targeting region of CDK8 along with miR-16 mimic or control. Luciferase activity assay was used to determine whether miR-16 target CDK8. (C) qPCR was used to detect the CDK8 level after miR-16 mimic or mimic control transfection. (D) Western blot was used to evaluate the protein expression of CDK8. (E) IHC and (F, G) QPCR was used to evaluate the expression level of CDK8 in NSCLC tissues and cell lines. (H, I) The correlation analysis was performed between XIST and miIR-16 along with miR-16 and CDK8 expression levels. *P < 0.05 versus normal/mimic control group.

member of cyclin-dependent kinase (CDK) family which play critical roles in cell cycle transitions and transcription or RNA splicing, we found that CDK8 was also a direct target gene of miR-16. Furthermore, there exist a positive correlation between the expression of XIST and CDK8. These findings exert as ceRNA relationship between XIST and CDK8.

In conclusion, we found that XIST promoted proliferation and migration of NSCLC. Further mechanism research firstly indicated that XIST up-regulated CDK8 via acting as a ceRNA of miR-16 in NSCLC. It provides a better understanding of the role of XIST and may contribute to the diagnose and therapy strategies in NSCLC.

The Wnt/β-catenin pathway is a conserved signaling pathway that is crucial for initiating and regulating a diverse range of biological processes, including embryogenesis, carcinogen-esis, cell growth, apoptosis, and cell polarity. CDK8 can directly regulate β-catenin-activated transcription including MED12, MED13 and its cyclin cofactor cyclin C. We will further explore the role of XIST and whether it regulates Wnt/β-catenin pathway.

Disclosure of conflict of interest

None.

Address correspondence to: Yushang Cui, Department of Thoracic Surgery, Peking Union Medical College Hospital, 1 Shuaifuyuan, Wangfujing, Dongcheng, Beijing 100730, P. R. China. E-mail: cyspeking@aliyun.com

References

[1] Ettinger DS, Akerley W, Borghaei H, Chang AC, Cheney RT, Chirieac LR, D'Amico TA, Demmy TL, Govindan R, Grannis FW Jr, Grant SC, Horn L, Jahan TM, Komaki R, Kong FM, Kris MG,

Krug LM, Lackner RP, Lennes IT, Loo BW Jr, Martins R, Otterson GA, Patel JD, Pinder-Schenck MC, Pisters KM, Reckamp K, Riely GJ, Rohren E, Shapiro TA, Swanson SJ, Tauer K, Wood DE, Yang SC, Gregory K, Hughes M; National comprehensive cancer network. Non-small cell lung cancer, version 2.2013. J Natl Compr Canc Netw 2013; 11: 645-653; quiz 653.

[2] Gettinger S, Lynch T. A decade of advances in treatment for advanced non-small cell lung cancer. Clin Chest Med 2011; 32: 839-51.

[3] Herbst RS, Heymach JV, Lippman SM. Lung cancer. N Engl J Med 2008; 359: 1367-1380.

[4] Wood SL, Pernemalm M, Crosbie PA, Whetton AD. The role of the tumor-microenvironment in lung cancer-metastasis and its relationship to potential therapeutic targets. Cancer Treat Rev 2014; 40: 558-566.

[5] Jemal A, Bray F, Center MM, Ferlay J, Ward E, Forman D. Global cancer statistics. CA Cancer J Clin 2011; 61: 69-90.

[6] Yang L, Froberg JE, Lee JT. Long noncoding RNAs: fresh perspectives into the RNA world. Trends Biochem Sci 2014; 39: 35-43.

[7] Clemson CM, Hutchinson JN, Sara SA, Ensminger AW, Fox AH, Chess A, Lawrence JB. An architectural role for a nuclear noncoding RNA: NEAT1 RNA is essential for the structure of paraspeckles. Mol Cell 2009; 33: 717-726.

[8] Kogo R, Shimamura T, Mimori K, Kawahara K, Imoto S, Sudo T, Tanaka F, Shibata K, Suzuki A, Komune S, Miyano S, Mori M. Long noncoding RNA HOTAIR regulates polycomb-dependent chromatin modification and is associated with poor prognosis in colorectal cancers. Cancer Res 2011; 71: 6320-6326.

[9] Youness RA, Gad MZ. Long non-coding RNAs: Functional regulatory players in breast cancer. Noncoding RNA Res 2019; 4: 36-44.

[10] Wang J, Zhang X, Chen W, Hu X, Li J, Liu C. Regulatory roles of long noncoding RNAs implicated in cancer hallmarks. Int J Cancer 2019; [Epub ahead of print].

[11] Sarfi M, Abbastabar M, Khalili E. Long noncoding RNAs biomarker-based cancer assessment. J Cell Physiol 2019; 234: 16971-16986.

[12] Fernandes JCR, Acuña SM, Aoki JI, Floeter-Winter LM, Muxel SM. Long non-coding RNAs in the regulation of gene expression: physiology and disease. Noncoding RNA 2019; 5.

[13] Wang X, Zhang G, Cheng Z, Dai L, Jia L, Jing X, Wang H, Zhang R, Liu M, Jiang T, Yang Y, Yang M. Knockdown of LncRNA-XIST suppresses proliferation and TGF-beta1-induced EMT in NSCLC through the Notch-1 pathway by regulation of miR-137. Genet Test Mol Biomarkers 2018; 22: 333-342.

[14] Li C, Wan L, Liu Z, Xu G, Wang S, Su Z, Zhang Y, Zhang C, Liu X, Lei Z, Zhang HT. Long non-coding RNA XIST promotes TGF-beta-induced epithelial-mesenchymal transition by regulating miR-367/141-ZEB2 axis in non-small-cell lung cancer. Cancer Lett 2018; 418: 185-195.

[15] Jiang H, Zhang H, Hu X, Li W. Knockdown of long non-coding RNA XIST inhibits cell viability and invasion by regulating miR-137/PXN axis in non-small cell lung cancer. Int J Biol Macromol 2018; 111: 623-631.

[16] Sun W, Zu Y, Fu X, Deng Y. Knockdown of lncRNA-XIST enhances the chemosensitivity of NSCLC cells via suppression of autophagy. Oncol Rep 2017; 38: 3347-3354.

[17] Wang H, Shen Q, Zhang X, Yang C, Cui S, Sun Y, Wang L, Fan X, Xu S. The long non-coding RNA XIST controls non-small cell lung cancer proliferation and invasion by modulating miR-186-5p. Cell Physiol Biochem 2017; 41: 2221-2229.

[18] Fang J, Sun CC, Gong C. Long noncoding RNA XIST acts as an oncogene in non-small cell lung cancer by epigenetically repressing KLF2 expression. Biochem Biophys Res Commun 2016; 478: 811-7.

[19] Ambros V. The functions of animal microRNAs. Nature 2004; 431: 350-355.

[20] Zanetti KA, Haznadar M, Welsh JA, Robles AI, Ryan BM, McClary AC, Bowman ED, Goodman JE, Bernig T, Chanock SJ, Harris CC. 3'-UTR and functional secretor haplotypes in mannose-binding lectin 2 are associated with increased colon cancer risk in African Americans. Cancer Res 2012; 72: 1467-1477.

[21] Ma L, Zhou Y, Luo X, Gao H, Deng X, Jiang Y. Long non-coding RNA XIST promotes cell growth and invasion through regulating miR-497/MACC1 axis in gastric cancer. Oncotarget 2017; 8: 4125-4135.

[22] Zhuang LK, Yang YT, Ma X, Han B, Wang ZS, Zhao QY, Wu LQ, Qu ZQ. MicroRNA-92b promotes hepatocellular carcinoma progression by targeting Smad7 and is mediated by long non-coding RNA XIST. Cell Death Dis 2016; 7: e2203.

[23] Yao Y, Ma J, Xue Y, Wang P, Li Z, Liu J, Chen L, Xi Z, Teng H, Wang Z, Li Z, Liu Y. Knockdown of long non-coding RNA XIST exerts tumor-suppressive functions in human glioblastoma stem cells by up-regulating miR-152. Cancer Lett 2015; 359: 75-86.

[24] Li C, Wan L, Liu Z, Xu G, Wang S, Su Z, Zhang Y, Zhang C, Liu X, Lei Z, Zhang HT. Long non-coding RNA XIST promotes TGF-beta-induced epithelial-mesenchymal transition by regulating miR-367/141-ZEB2 axis in non-small-cell lung cancer. Cancer Lett 2018; 418: 185-195.

[25] Wang Y, Liang Y, Luo J, Nie J, Yin H, Chen Q, Dong J, Zhu J, Xia J, Shuai W. XIST/miR-139 axis regulates bleomycin (BLM)-induced extracellular matrix (ECM) and pulmonary fibrosis

through beta-catenin. Oncotarget 2017; 8: 65359-65369.

[26] Wang H, Shen Q, Zhang X, Yang C, Cui S, Sun Y, Wang L, Fan X, Xu S. The long non-coding RNA XIST controls non-small cell lung cancer proliferation and invasion by modulating miR-186-5p. Cell Physiol Biochem 2017; 41: 2221-2229.

[27] Feng QQ, Dong ZQ, Zhou Y, Zhang H, Long C. miR-16-1-3p targets TWIST1 to inhibit cell proliferation and invasion in NSCLC. Bratisl Lek Listy 2018; 119: 60-65.

[28] Wang H, Zhang Y, Wu Q, Wang YB, Wang W. miR-16 mimics inhibit TGF-beta1-induced epithelial-to-mesenchymal transition via activation of autophagy in non-small cell lung carcinoma cells. Oncol Rep 2018; 39: 247-254.

[29] Wang W, Chen J, Dai J, Zhang B, Wang F, Sun Y. MicroRNA-16-1 inhibits tumor cell proliferation and induces apoptosis in A549 non-small cell lung carcinoma cells. Oncol Res 2016; 24: 345-351.

[30] Firestein R, Bass AJ, Kim SY, Dunn IF, Silver SJ, Guney I, Freed E, Ligon AH, Vena N, Ogino S, Chheda MG, Tamayo P, Finn S, Shrestha Y, Boehm JS, Jain S, Bojarski E, Mermel C, Barretina J, Chan JA, Baselga J, Tabernero J, Root DE, Fuchs CS, Loda M, Shivdasani RA, Meyerson M, Hahn WC. CDK8 is a colorectal cancer oncogene that regulates beta-catenin activity. Nature 2008; 455: 547-551.

[31] Brägelmann J, Klümper N, Offermann A, von Mässenhausen A, Böhm D, Deng M, Queisser A, Sanders C, Syring I, Merseburger AS, Vogel W, Sievers E, Vlasic I, Carlsson J, Andrén O, Brossart P, Duensing S, Svensson MA, Shaikhibrahim Z, Kirfel J, Perner S. Pan-cancer analysis of the mediator complex transcriptome identifies CDK19 and CDK8 as therapeutic targets in advanced prostate cancer. Clin Cancer Res 2017; 23: 1829-1840.

[32] Broude EV, Győrffy B, Chumanevich AA, Chen M, McDermott MS, Shtutman M, Catroppo JF, Roninson IB. Expression of CDK8 and CDK8-interacting genes as potential biomarkers in breast cancer. Curr Cancer Drug Targets 2015; 15: 739-749.

[33] Firestein R, Bass AJ, Kim SY, Dunn IF, Silver SJ, Guney I, Freed E, Ligon AH, Vena N, Ogino S, Chheda MG, Tamayo P, Finn S, Shrestha Y, Boehm JS, Jain S, Bojarski E, Mermel C, Barretina J, Chan JA, Baselga J, Tabernero J, Root DE, Fuchs CS, Loda M, Shivdasani RA, Meyerson M, Hahn WC. CDK8 is a colorectal cancer oncogene that regulates beta-catenin activity. Nature 2008; 455: 547-551.

[34] Seo JO, Han SI, Lim SC. Role of CDK8 and beta-catenin in colorectal adenocarcinoma. Oncol Rep 2010; 24: 285-291.